OPTOELECTRONICS AND ADVANCED MATERIALS – RAPID COMMUNICATIONS Vol. 4, No. 5, May 2010, p. 624 - 629

Bidirectional dual-channel chaos synchronization and communication based on mutually coupled VCSELs with optical feedback

LI-HUA DU[a], ZHENG-MAO WU[a,b], TAO DENG[a], GUANG-QIONG XIA[a,b*]
[a]*School of Physics, Southwest University, Chongqing 400715, China*
[b]*State key Lab of Millimeter Waves, Southeast University, Nanjing 210096, China*

Based on mutually coupled vertical-cavity surface-emitting lasers (VCSELs) with optical feedback, a bidirectional dual-channel chaos security communication system are proposed and theoretically investigated. The results show that, through selecting suitable system parameters, high-quality isochronal synchronization can be obtained for the *x*-, *y*-LP mode as well as the total intensities, respectively; the synchronization performances for each LP mode and the total intensities preserve a certain extent tolerance to intrinsic mismatched parameters except they are sensitive to frequency detuning between the two VCSELs. Based on the chaos synchronization of the *x*- and *y*-LP modes, bidirectional dual-channel communication performances have been preliminarily examined under two encryption methods, namely chaos masking (CMS) and additive chaos modulation (ACM).

(Received January 21, 2010; accepted May 20, 2010)

Keywords: Vertical-cavity surface-emitting laser (VCSEL), Chaos synchronization, Dual-channel, Bidirectional communication

1. Introduction

Chaos synchronization and secure communication based on semiconductor lasers have attracted considerable interests during the recent twenty years [1-25]. As one of the microchip lasers, VCSELs exhibit many advantages compared to conventional edge-emitting semiconductor lasers (EELs), such as low threshold current, circular output beam with narrow divergence, intrinsically single-longitudinal mode, low cost and large-scale integration into two-dimensional arrays. An obvious difference between VCSELs and EELs is that the output of VCSELs maybe exist two orthogonal linear polarization (LP) modes (i. e., x- and y- LP modes) because of the weak material and cavity anisotropies, which inevitably results in more complex dynamic behaviors for a VCSEL under external disturbance [14-19] than those happens in a EEL under external disturbance. In recent years, the synchronization characteristics for each LP mode in VCSELs based on unidirectionally coupled systems have been investigated [14-17]. Meantime, chaos synchronization between mutually coupled VCSELs without optical feedback have already been studied experimentally [18, 20] and theoretically [19, 21]. However, relevant reports have shown that the chaos synchronization between two mutually coupled VCSELs without optical feedback, is not stable, and the leader/laggard synchronization is usually observed in a time dependent manner. In order to obtain stable mutual isochronal chaotic synchronization, optical feedback has been introduced into the mutually coupled system [22]. After neglecting polarization properties in the VCSELs, chaos synchronization and related communication performances for total output intensity of mutually coupled VCSELs with optical feedback has been checked [22, 23]. In this paper, a novel bidirectional dual-channel chaos security communication system based on mutually coupled VCSELs with optical feedback is proposed, and chaos synchronization characteristics for each LP mode and the total intensities, together with the influence of mismatched parameters on the synchronization quality, are analyzed based on spin-flip model (SFM) [26]. Furthermore, the communication related performances of dual-channel messages encoded respectively in two LP modes have been briefly examined under chaos masking (CMS) and additive chaos modulation (ACM) encryption schemes.

2. Systematical configuration and theory

The schematic diagram of bidirectional dual-channel chaos security system based on mutually coupled VCSELs with optical feedback is depicted in Fig. 1. The outputs of two mutually coupled lasers VCSEL1 and VCSEL2 include two orthogonal LP modes (*i. e.*, *x*- and *y*- LP modes). The output of VCSEL1 is divided into two beams by a non-polarizing beam splitter (BS1). One part is separated into *x*- and *y*-LP modes by a polarizing beam splitter (PBS2) so that different messages m_x and m_y can be encoded respectively upon each LP mode, and then the *x*- and *y*-LP modes recombined in PBS3. The recombined beam is separated by BS2, where one part is fed back to VCSEL1 and the other is injected into VCSEL2. It should be pointed out that above message encoded model is just suitable for ACM encryption scheme. For CMS encryption scheme, the optical path from BS2 to M4 is replaced by

the path from BS2' to M4', and BS2, VA1, M4 are accordingly replaced by BS2', VA1', M4'; The other part of the output from VCSEL1 is divided into *x*- and *y*-LP modes by PBS1, and then they are directly detected by two photo detectors (PD1 and PD2), respectively. The injected power from VCSEL1 to VCSEL2 is also divided into two parts by BS4. One part is coupled into VCSEL2, the other is separated into two LP modes by PBS8 and then they are detected by PD7 and PD8, respectively. Variable attenuators (VAs) are used to adjust feedback or coupling strength, optical isolators (ISOs) ensure the light unidirectional transmission, and fourth-Butterworth low-pass filters (FBFs) are used to improve the performance of demodulation. The output of VCSEL2 undergoes similar processes as that of VCSEL1, and the messages encoded upon the *x*- and *y*-LP modes of VCSEL2 are m_x' and m_y', respectively.

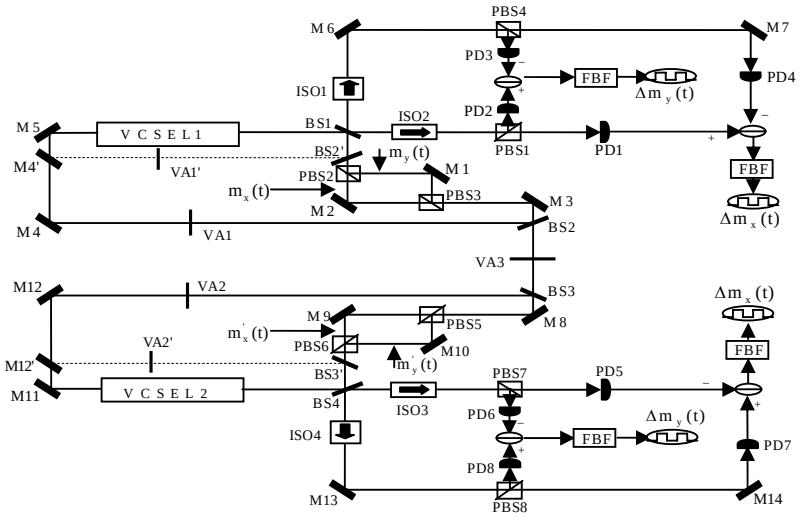

Fig. 1. Bidirectional dual-channel chaos security system based on mutually coupled VCSELs with optical feedback. BS: Non-polarizing beam splitter; PBS: Polarizing beam splitter; M: Mirror; ISO: Isolator; PD: Photo detector; FBF: Fourth-Butterworth low-pass filter; VA: Variable attenuator.

Based on SFM [26], the rate equations for each VCSEL can be described by [15, 16]:

$$\frac{dE_x^{1,2}}{dt} = k^{1,2}(1+i\alpha^{1,2})(N^{1,2}E_x^{1,2} + in^{1,2}E_y^{1,2} - E_x^{1,2}) - (\gamma_a^{1,2} + i\gamma_p^{1,2})E_x^{1,2} + F_x^{1,2} + \eta_{inj}E_x^{2,1}(t-\tau_{inj})\exp[-i2\pi(\nu^{2,1}\tau_{inj} - \Delta\nu^{21,12}t)] + \eta_f E_x^{1,2}(t-\tau_f)\exp(-i2\pi\nu^{1,2}\tau_f) \quad (1)$$

$$\frac{dE_y^{1,2}}{dt} = k^{1,2}(1+i\alpha^{1,2})(N^{1,2}E_y^{1,2} - in^{1,2}E_x^{1,2} - E_y^{1,2}) + (\gamma_a^{1,2} + i\gamma_p^{1,2})E_y^{1,2} + F_y^{1,2} + \eta_{inj}E_y^{2,1}(t-\tau_{inj})\exp[-i2\pi(\nu^{2,1}\tau_{inj} - \Delta\nu^{21,12}t)] + \eta_f E_y^{1,2}(t-\tau_f)\exp(-i2\pi\nu^{1,2}\tau_f) \quad (2)$$

$$\frac{dN^{1,2}}{dt} = -\gamma_e^{1,2}N^{1,2}(1+\left|E_x^{1,2}\right|^2 + \left|E_y^{1,2}\right|^2) + \gamma_e^{1,2}\mu^{1,2} - i\gamma_e^{1,2}n^{1,2}(E_y^{1,2}E_x^{1,2}* - E_x^{1,2}E_y^{1,2}*) \quad (3)$$

$$\frac{dn^{1,2}}{dt} = -\gamma_s^{1,2}n^{1,2} - \gamma_e^{1,2}n^{1,2}(\left|E_x^{1,2}\right|^2 + \left|E_y^{1,2}\right|^2) - i\gamma_e^{1,2}N^{1,2}(E_y^{1,2}E_x^{1,2}* - E_x^{1,2}E_y^{1,2}*) \quad (4)$$

where superscripts *1* and *2* stand for two mutually coupled VCSELs, respectively, and subscripts *x* and *y* stand for *x*- and *y*-LP modes, respectively. E is the slowly varying amplitude of field, N is total inversion population, and n is the difference between population inversions of opposite spins, κ is the field decay rate, γ_e is the carrier decay rate, and γ_s is the spin-flip rate, μ is the normalized injection current, α is the linewidth enhancement factor, γ_a and γ_p are the linear anisotropies representing dichroism and birefringence, respectively, η_f is the feedback rate, η_{inj} is the injection rate, τ_f is the feedback delay time, τ_{inj} is the propagation time, v is the frequency of free-running VCSEL, and $\Delta v^{21}=-\Delta v^{12}=v^2-v^1$ is the frequency detuning. F accounts for the Langevin noise sources associated to spontaneous emission processes, and

$$F_x^{1,2} = \sqrt{\beta_{sp}^{1,2}/2}\,(\sqrt{N^{1,2}+n^{1,2}}\,\xi_1^{1,2} + \sqrt{N^{1,2}-n^{1,2}}\,\xi_2^{1,2}) \quad (5a)$$

$$F_y^{1,2} = -i\sqrt{\beta_{sp}^{1,2}/2}\,(\sqrt{N^{1,2}+n^{1,2}}\,\xi_1^{1,2} - \sqrt{N^{1,2}-n^{1,2}}\,\xi_2^{1,2}) \quad (5b)$$

where ξ_1 and ξ_2 indicate independent Gaussian white noise with zero mean and unitary variance, and β_{sp} is spontaneous emission rate [24].

3. Results and discussion

3.1 Complete chaos synchronization

Eqs. (1)- (4) can be numerically solved by the fourth-order Runge-Kutta method. Firstly, we assume these two

VCSELs have the same device parameters and operating circumstance. During the simulation, the used parameters are: $\alpha^1=\alpha^2=3$, $\kappa^1=\kappa^2=300$GHz, $\gamma_e^{\,1}=\gamma_e^{\,2}=1$GHz, $\gamma_a^{\,1}=\gamma_a^{\,2}=0.1$GHz, $\gamma_p^{\,1}=\gamma_p^{\,2}=6$GHz, $\gamma_s^{\,1}=\gamma_s^{\,2}=50$GHz, $\nu^1=\nu^2=3.53\times10^{14}$Hz (the corresponding central wavelength is 850 nm), $\beta_{sp}=1\times10^{-6}$GHz, $\tau_f=\tau_{inj}=4$ns, $\mu^1=\mu^2=1.3$, $\eta_f=\eta_{inj}=9$GHz.

To specifically describe the synchronization quality between these two lasers, the quality of chaos synchronization and its time shift for each LP mode and the total intensities can be quantified by calculating the following shifted correlation coefficients [24, 25]:

$$\rho_i(\Delta t)=\frac{\langle[I_i^1(t)-\langle I_i^1(t)\rangle]\cdot[I_i^2(t-\Delta t)-\langle I_i^2(t)\rangle]\rangle}{\sqrt{\langle\left|I_i^1(t)-\langle I_i^1(t)\rangle\right|^2\rangle\cdot\langle\left|I_i^2(t)-\langle I_i^2(t)\rangle\right|^2\rangle}} \tag{6}$$

where subscript $i=x$, y and total refer to the x-, y-LP mode and the total intensities, respectively. $I_x=|E_x|^2$, $I_y=|E_y|^2$, $I_{total}=|E_x|^2+|E_y|^2$, Δt is the time shift, and the brackets $\langle\cdot\rangle$ denote the temporal averaging.

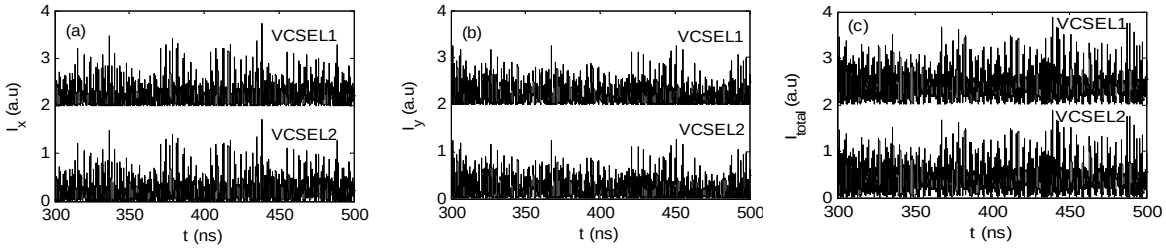

Fig. 2. Output time series of x-, y-LP mode and the total intensities, where the upper and the lower traces correspond to VCSEL1 and VCSEL2, respectively.

Fig. 2 gives the time series of the x-, y-LP mode and the total intensities of VCSEL1 and VCSEL2, respectively, where the upper and the lower traces correspond to the output of VCSEL1 and VCSEL2, respectively. From this diagram, it can be seen that the output of both lasers are the mixed LP modes (including x- and y-LP modes), and the output intensities of each LP mode and the total intensities display chaos dynamics.

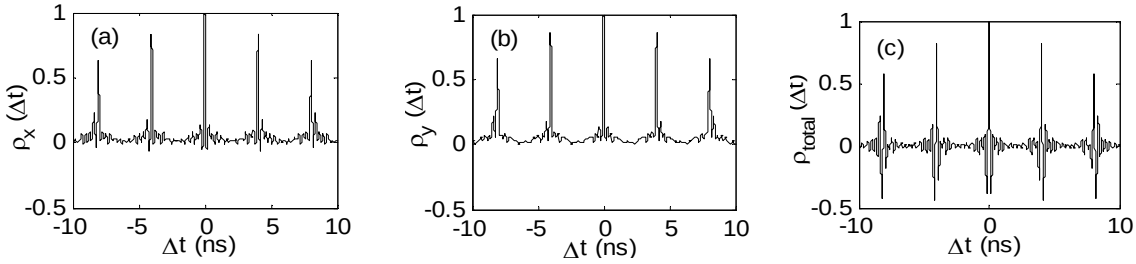

Fig. 3. Correlation coefficients between mutually coupled VCSELs, where (a), (b) and (c) are the correlation coefficients of x-, y-LP mode and the total intensities, respectively.

Fig. 3 gives the correlation coefficients ρ_x, ρ_y, and ρ_{total} between these two VCSELs. As shown in this diagram, high synchronization quality with the maximum of the correlation coefficients above 0.99 can be obtained with zero time-lag for each LP mode as well as the total intensities of the two lasers.

3.2 Influence of the mismatched parameters on synchronization quality

It is well known that in order to achieve complete synchronization, it is quite important to match corresponding parameters of the two VCSELs. However, it is impossible to attain perfect matching in practice. Therefore, it is essential to investigate the influences of mismatched parameters on the quality of chaos synchronization. For convenience, we fix parameters of VCSEL1, and only change the parameters of VCSEL2. The relative intrinsic mismatched parameters are defined as [16]:

$$\Delta\gamma_a=(\gamma_a^{\,2}-\gamma_a^{\,1})/\gamma_a^{\,1},\ \Delta\gamma_s=(\gamma_s^{\,2}-\gamma_s^{\,1})/\gamma_s^{\,1},\ \Delta\gamma_p=(\gamma_p^{\,2}-\gamma_p^{\,1})/\gamma_p^{\,1},$$
$$\Delta\gamma_e=(\gamma_e^{\,2}-\gamma_e^{\,1})/\gamma_e^{\,1},\ \Delta\alpha=(\alpha^2-\alpha^1)/\alpha^1,\ \Delta\kappa=(\kappa^2-\kappa^1)/\kappa^1 \tag{7}$$

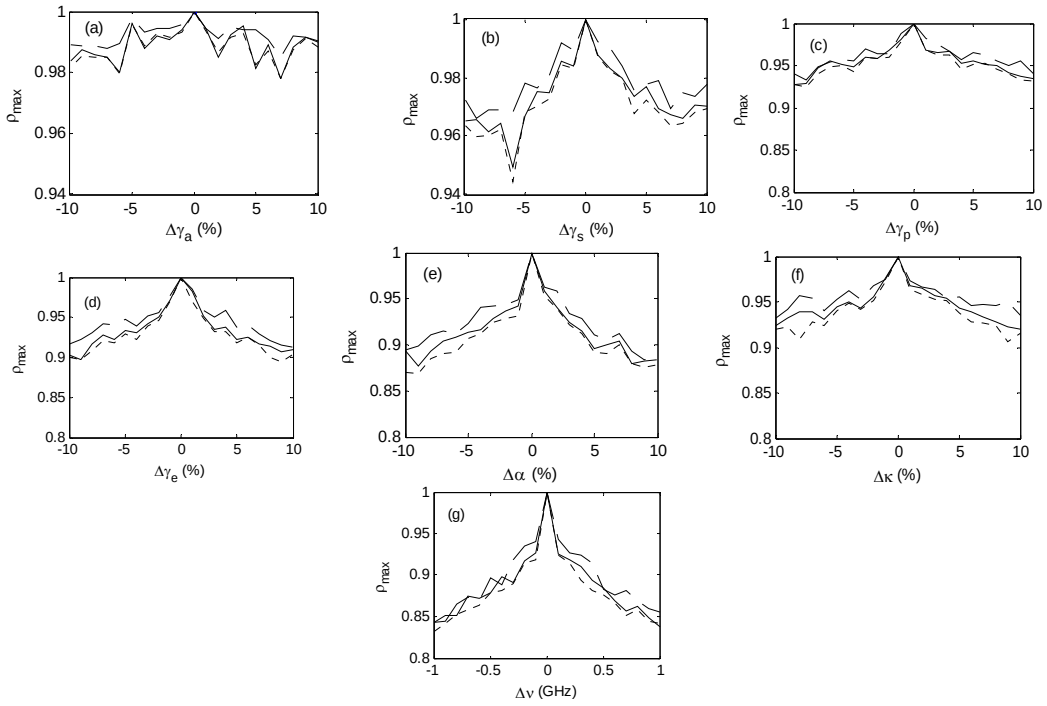

Fig. 4. Maximum correlation coefficients as a function of various mismatched parameters, where solid, dashed and dotted lines correspond to the x-LP, y-LP and total intensities, respectively.

Fig. 4 shows the variation of the maximum correlation coefficients of *x*-, *y*-LP mode and the total intensities with the intrinsic mismatched parameters and frequency detuning $\Delta\nu$. From this diagram, it can be observed that the maximum correlation coefficients of each mode and the total intensities preserve above 0.94 for $\Delta\gamma_a$ and $\Delta\gamma_s$ varying from -10% to 10% (see (a) and (b)), the influence of $\Delta\gamma_a$ is the smallest and the influence of $\Delta\alpha$ is the largest in all intrinsic mismatched parameters. The influences of $\Delta\gamma_p$, $\Delta\gamma_e$ and $\Delta\kappa$ on the synchronization quality are relative larger than that of $\Delta\gamma_a$ and $\Delta\gamma_s$, but the correlation coefficients can still be maintained above 0.89. As shown in Fig. 4 (g), frequency detuning $\Delta\nu$ extensively affects the synchronization quality.

3.3 Message encoding and decoding

Based on above results, this proposed chaos system has good synchronization performances for both two LP modes. In this section, we will preliminarily examine bidirectional dual-channel communication ability of this system by using these two LP modes. Different encoding and decoding techniques such as chaos shift keying (CSK), chaos masking (CMS) and chaos modulation (CM) have been proposed and investigated for secure message transmission based on chaotic synchronization [6, 27]. In this paper, we will test the communication performances in each LP mode under CMS and ACM schemes, respectively. The modulation depth of message is fixed to 5%, and the message transmission rate is 500Mbits/s.

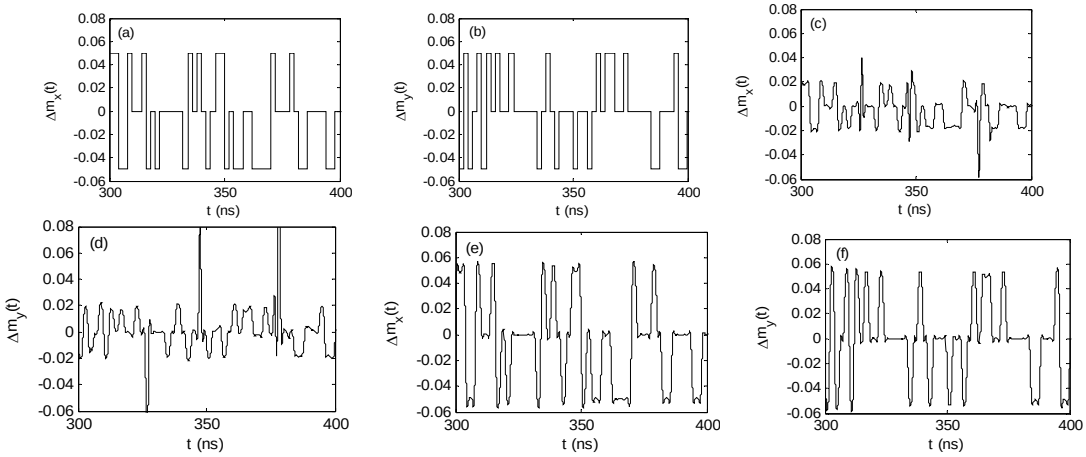

Fig. 5. Encoding message differences and decoding message differences under perfect matching case, where the left and right volumes correspond to the x- and y-LP modes, respectively, (a) and (b) are original message differences, (c) and (d) are recovered message differences under CMS, (e) and (f) are recovered message differences under ACM.

Firstly, we consider perfect matching case. In Fig. 5 (a) and (b) display the differences between the original messages ($\Delta m_{x,y}(t)=m_{x,y}(t-\Delta t)-m'_{x,y}(t)$) encoded upon *x*- and *y*-LP modes, (c) and (d) are the corresponding recovered message differences under CMS scheme, and (e) and (f) are the corresponding recovered message differences under ACM scheme. One can see that under perfect matching condition, message recovery is poor under CMS scheme but is satisfactory under ACM scheme. The reason is that message encoding destroys the symmetry of this system under CMS scheme, while the symmetry can be maintained under ACM scheme.

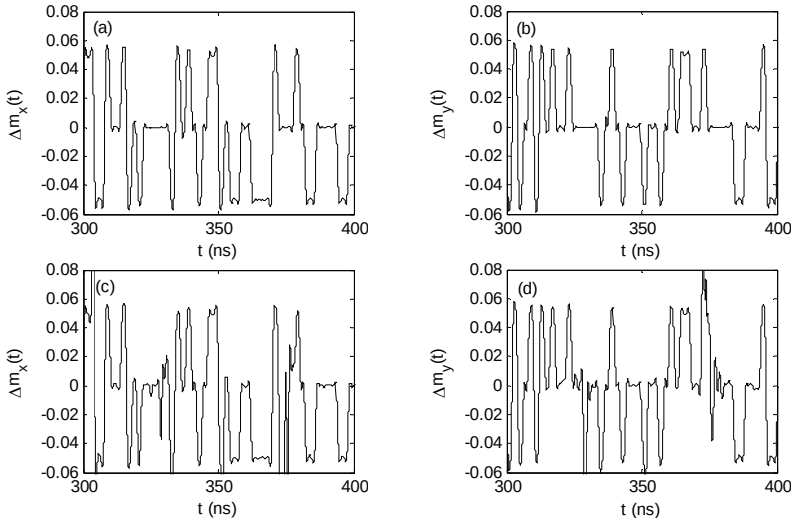

Fig. 6. Decoding message differences under ACM encryption scheme for Δγa =2% ((a) and (b)) and Δγe=2% ((c) and (d)), where the left and right volumes correspond to the x- and y-LP modes, respectively.

Next, we take 2% of mismatched parameters $\Delta\gamma_a$ and $\Delta\gamma_e$ as an example to investigate the influence of intrinsic mismatched parameters on message transmission performances. Under ACM encryption scheme, the corresponding decoded results are shown in Fig. 6, where the original messages are the same as those of Fig. 5. As shown in these figures, the message encoded upon each LP mode can still be recovered successfully under suitable mismatched parameters case, and the decoded effects for $\Delta\gamma_e$ are relatively inferior to that for $\Delta\gamma_a$ due to that the influence of $\Delta\gamma_e$ on synchronization quality is relatively larger than that of $\Delta\gamma_a$.

4. Conclusions

In conclusion, a novel bidirectional dual-channel chaos synchronization and communication system has been proposed and investigated. In this system, based on the chaos synchronization of two LP modes (*x*- and *y*-LP modes) in mutually coupled VCSELs with optical feedback, bidirectional dual-channel security communication may be realized. The results show that high quality and stable chaos synchronization can be obtained for each LP mode as well as the total intensities under perfect matching case. The synchronization quality will decrease with the increase of the parameters mismatching degree, and a certain extent tolerance to intrinsic mismatched parameters can be maintained for mismatched parameters varied within ±10%. It should be noticed that synchronization quality is very sensitive to frequency detuning between the two VCSELs, and the frequency detuning should be smaller than 0.3 GHz to obtain correlation coefficient above 0.9. Furthermore, bidirectional dual-channel communication performances have been investigated for 500 Mbits/s message. The messages encoding upon *x*- and *y*-LP modes respectively, can be extracted successfully under ACM scheme but cannot be recovered under CMS scheme. Additionally, the communication performance will be affected by the mismatched parameters, but the effect is not very serious.

Acknowledgements

This work was supported by the National Natural Science Foundation of China under Grant No. 60978003, the Open Fund of the State Key Lab of Millimeter Waves of China and the Special Funds of Southwest University for Basic Scientific Research in Central Universities.

References

[1] K. Kusumoto, J. Ohtsubo, Opt. Lett. **27**, 989 (2002).
[2] W. L. Zhang, W. Pan, B. Luo, X. H. Zou, M. Y. Wang, Z. Zhou, Opt. Lett. **33**, 237 (2008).
[3] J. Paul, S. Sivaprakasam, K. A. Shore, J. Opt. Soc. Am. B **21**, 514 (2004).
[4] R. Vicente, C. R. Mirasso, I. Fischer, Opt. Lett. **32**,

403 (2007).
[5] T. Deng, G. Q. Xia, L. P. Cao, J. G. Chen, X. D. Lin, Z. M. Wu, Opt. Commun. **282**, 2243 (2009).
[6] J. M. Liu, H. F. Chen, S. Tang, IEEE J. Quantum Electron. **38**, 1184 (2002).
[7] T. Heil, I. Fischer, W. Elsasser, J. Mulet, C. R. Mirasso, Phys. Rev. Lett. **86**, 795 (2001).
[8] H. Fujino, J. Ohtsubo, Opt. Rev. **8**, 351 (2001).
[9] J. Mulet, C. Mirasso, T. Heil, I. Fischer, J. Opt. B: Quantum Semiclass. Opt. **6**, 97 (2004).
[10] N. Gross, W. Kinzel, I. Kanter, M. Rosenbluh, L. Khaykovich, Opt. Commun. **267**, 464 (2006).
[11] E. Klein, N. Gross, E. Kopelowitz, M. Rosenbluh, L. Khaykovich, W. Kinzel, I. Kanter, Phys. Rev. E **74**, 046201 (2006).
[12] I. B. Schwartz, L. B. Shaw, Phys. Rev. E **75**, 046207 (2007).
[13] G. Q. Xia, Z. M. Wu, J. G. Wu, Opt. Express **13**, 3445 (2005).
[14] Y. Hong, P. S. Spencer, S. Bandyopadhyay, P. Rees, K. A. Shore, Opt. Commun. **216**, 185 (2003).
[15] D. Z. Zhong, G. Q. Xia, Z. M. Wu, X. H. Jia, Opt. Commun. **281**, 1698 (2008).
[16] D. Z. Zhong, Z. M. Wu, Opt. Commun. **282**, 1631 (2009).
[17] J. Liu, Z. M. Wu, G. Q. Xia, Opt. Express **17**, 12619 (2009).
[18] N. Fujiwara, Y. Takiguchi, J. Ohtsubo, Opt. Lett. **28**, 1677 (2003).
[19] K. Panajotov, A. Uchida, M. Sciamanna, in CLEO/Europe and IQEC 2007 Conference Digest, paper JSI_5, June 20, 1, 2007.
[20] A. Uchida, H. Someya, M. Ozaki, K. Tanaka, S. Yoshimori, K. Panajotov, M. Sciamanna, IEEE/LEOS Winter Topical Meeting Series on Nonlinear Dynamics in Photonic System, Jan. 2009, 126.
[21] K. Panajotov, M. Sciamanna, H. Thienpont, A. Uchida, Opt. Lett. **33**, 3031 (2008).
[22] N. Jiang, W. Pan, L. S. Yan, B. Luo, L. Yang, S. Y. Xiang, D. Zheng, Opt. Commun. **282**, 2217 (2009)
[23] N. Jiang, W. Pan, B. Luo, W. L. Zhang, D. Zheng, Chin. Opt. Lett. **6**, 517 (2008).
[14] I. Gatare, M. Sciamanna, A. Locquet, K. Panajotov, Opt. Lett. **32**, 1629 (2007).
[15] G. Q. Xia, Z. M. Wu, J. F. Liao, Opt. Commun. **282**, 1009 (2009).
[16] J. M. Regalado, F. Prati, M. S. Miguel, N. B. Abraham, IEEE J. Quantum Electron. **33**, 765 (1997).
[17] S. Tang, J. M. Liu, IEEE J. Quantum Electron. **39**, 1468 (2003).

*Corresponding author: gqxia@swu.edu.cn